Heliyon 10 (2024) e35091

Contents lists available at ScienceDirect

Heliyon

journal homepage: www.cell.com/heliyon

Research article

Effect of hot isostatic pressing on microstructure and properties of cooled hot dip aluminum coating in magnetic field

Li Yong [a,*], Xu Wei [a], Bai Jingfei [a], Su Qing [b], Xu RuTao [a], Liu Hong [a], Dan Yu [a]

[a] Chengdu Aeronautic Polytechnic, Chengdu, 610100, China
[b] Material Corrosion and Protection Key Laboratory of Sichuan Province, Zigong, 643000, China

ARTICLE INFO

Keywords:
Titanium alloy
Magnetic field
Coating
Hot isostatic pressing

ABSTRACT

The effect of hot isostatic pressing (HIP) on the microstructure and properties of hot dip aluminum coating cooled in a magnetic field was investigated in this study. In order to improve the microstructure and properties of magnetic dip aluminum coating, hot isostatic pressing technology was used for post-treatment. Initially, a traditional aluminum-impregnated coating was prepared on the surface of titanium alloy TA15, an alternating electromagnetic field was applied during the forming and solidification process of the coating. Finally, the coating was treated with hot isostatic pressing technology. Analyzed three different coatings of the microstructure and element distribution, and tested the microhardness of the coatings at various positions. The test results revealed that the TA15 titanium alloy hot-dip aluminum coatings obtained through the three different processes exhibited a gradient structure. Compared with the traditional hot-dipped aluminum air-cooled coating, when an appropriate intensity of alternating electromagnetic field was applied during the coating solidification process, the outer coating structure was enhanced, the number of holes was reduced, the microstructure density increased, and the number of cracks significantly decreased. The defects of the 800 °C hot isostatic magnetic cold and hot dip aluminum coating were repaired under high temperature and pressure, resulting in a uniform and fine microstructure. The comprehensive properties of the magnetic cold and hot dip aluminum coating on the surface of the titanium alloy were effectively enhanced through hot isostatic pressing.

1. Introduction

Titanium alloy materials are widely utilized in medical, transportation, aerospace, and other industries. Surface modification of titanium alloy materials has important practical significance, improve the surface hardness of alloy, but also improve its high temperature oxidation resistance, extend the service life of titanium alloy aviation equipment Hot dip aluminum (HDA) technology is to put titanium alloy into aluminum liquid at high temperature for thermal reaction, and then cool it in the airtoform a thin protective coating on the alloy surface [1–4]. The traditional hot dipping aluminum process is adapted to the surface of titanium alloy to form TixAly intermetallic compound gradient coating, which can improve its surface properties. However, due to the large difference in physical properties between the matrix alloy and pure aluminum materials, the difference in properties between the base material and the aluminum alloy will induce cracks and other defects in the coating, which limits the engineering practicality of this technology.

* Corresponding author.
E-mail address: 250571951@qq.com (L. Yong).

https://doi.org/10.1016/j.heliyon.2024.e35091
Received 31 May 2024; Received in revised form 7 July 2024; Accepted 23 July 2024
Available online 23 July 2024
2405-8440/© 2024 The Authors. Published by Elsevier Ltd. This is an open access article under the CC BY-NC license (http://creativecommons.org/licenses/by-nc/4.0/).

In order to solve the above problems, it is imperative toregulate the solidification process of the coating by applying an external field auxiliary means. Alternating electromagnetic fields can control the convection of liquid metal in the coating, reducing the number of cracks and refining the grains [5–10]. Li Sinian [11]prepared a high-entropy alloy coating materials using applied magnetic field assisted plasma cladding technology. It was found that the microhardness and wear resistance of high-entropy alloy coating were improved under the assistance of different magnetic fields of stable magnetic field and alternating magnetic field. Chen Long et al. [12] adopted alternating magnetic field with a certain intensity to assist laser cladding of 304 stainless steel powder. As the intensity of alternating magnetic field increased, the grain structure became finer, and the hardness of the cladding layer increased too. Gatzen et al. [13]studied the influence and mechanism of electromagnetic agitation in the process of electromagnetic field-assisted laser welding technology and believed that the applied electromagnetic field could control the flow of melt and make the solute elements periodically distributed. The use of electromagnetic stirring technology alone is insufficient to meet the requirements of the aerospace field in controlling coating defects. Hot isostatic pressing technology is a process, in which high temperature and high-pressure work together. High temperature and pressure of the same phase cause phase transformation and interfacial reaction of powder alloys, which is often used in pyrometallurgy process and post-treatment of alloys to eliminate internal defects of materials [14–19]. Gao Yuxiang [20–22]conducted post-treatment on the test rod of Ti48Al2Cr2Nb alloy prepared by electron beam melting forming technology, and the results showed that the density and microhardness of the alloy increased after hot isostatic pressing treatment. Tian Xiaoying [23]carried out hot isostatic pressing treatment for metal-cast magnesium alloy, and believed that after hot isostatic pressing treatment, the alloy had fine grain structure, improved tensile strength and plasticity, and eliminated shrinkage porosity and shrinkage holes.

This paper introduces electromagnetic field into the solidification process of the coating, and uses the non-contact stirring effect of alternating electromagnetic field to suppress the number of coating defects, and then post-treats the coating in the hot isostatic pressing equipmentto repair the coating under a certain temperature and pressure [24–27]. Research on the application of electromagnetic field in the process of material preparation mainly focuses on the effect of magnetic field on the solidification structure of alloy. There are few reports on the solidification structure and thermal cracking behavior of coating under the action of electromagnetic field. Hot isostatic pressing technology is often used in powder metallurgy industry and post-treatment of special prepared alloys, and hot isostatic pressing technology is also very rare for post-hot pressing treatment of hot dipped aluminum coatings. In this paper, the electromagnetic field technology and hot isostatic pressing technology are applied to the hot dipping aluminum coating of titanium alloy, which is expected to eliminate the internal pores of the coating, improve its organizational structure, enhance the overall mechanical properties, and greatly extend the service life of aviation titanium alloy equipment [28–30].

2. Materials and methods

TA15 titanium alloy is the base material selected for this experiment, with dimensions of 20 mm × 20 mm × 5 mm. The surface of the alloy is polished, and cleaned with an ultrasonic cleaner. Use a resistance furnace to melt a block of industrial pure aluminum with a purity of 99.7 % at a temperature of 760 °C, and maintain the temperature for 30 min. The pre-treated TA15 titanium alloy is then immersed in the liquid aluminum, allowing the diffusion of Ti atoms and Al atoms to form a new phase at high temperatures. After 8 min, the coated TA15 titanium alloy is taken out and cooled in the air, serving as a traditional hot-dip aluminum sample. Additionally, the coated alloy is exposed to an alternating electromagnetic field of certain intensity until it reaches room temperature. This process yields the alloy intermediate sample and the contrast sample. The intermediate sample of cooled Hot Dip Aluminum Coating in Magnetic Field was put into the hot isostatic pressure testing machine, the air in the furnace was removed with a vacuum pump and the inert gas was introduced to prevent the coating from oxidizing during the heating process, the temperature in the furnace was set to the required temperature, the pressure of 30Mp was applied, the heat preservation and pressure were kept for 30 min, and the air cooling was quickly cooled to room temperature.

The experimental setup includes a magnetic field generating device, as shown in Fig. 1. It consists of a stainless-steel frame wrapped around the working coil and a voltage regulator. The stainless-steel generator, shown in Fig. 1 (a), is externally wound by the working coil and connected to the AC power supply, generating a contactless alternating electromagnetic field inside the generator. To protect the equipment from the high-temperature solution during the experiment, the outermost layer is covered by an asbestos cloth. Fig. 1

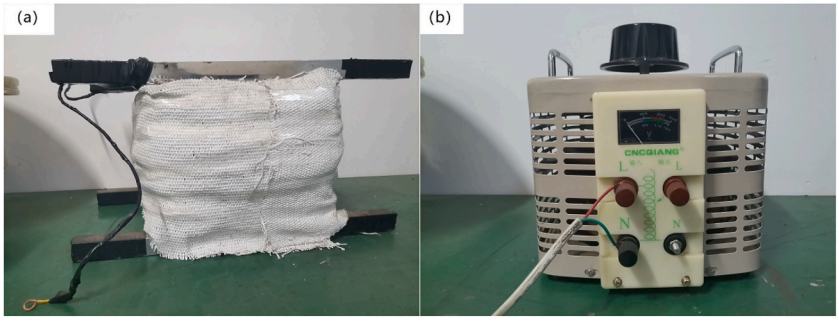

Fig. 1. (a) The stainless-steel generator; (b) The voltage regulator.

(b) depicts the voltage regulator model TDGC2-500 W, which adjusts the voltage intensity to control the intensity of the alternating electromagnetic field by altering the current intensity in the working coil. The current intensity of the magnetic field used in the experiment is 15 A and the frequency is 50HZ. The post-treatment process parameters using hot isostatic pressing technology are presented in Table 1.

The coating profile was cut into three groups of samples, which were then transformed into metallographic samples. After corrosion, the microstructure of the coating was observed. The morphology and microstructure of the coating section were observed by JSM-IT500 scanning electron microscope. The element distribution near the coating section was obtained by point scanning. The phase composition near the coating cross section was analyzed(XRD). Surface hardness testingwere conducted to measure the Vickers hardness at each longitudinal position of the coating. Five points were measured on each occasion, and the average value was considered as the final measurement result.

3. Results and discussion

3.1. Microstructure investigations

The microstructure of TA15 titanium alloy with a traditional hot-dipped aluminum air cooling pattern is shown in Fig. 2. The coating consists of a gradient structure, with the outermost layer being pure aluminum, followed by the outer coating and the binding layer from the outside to the inside. The surface of the substrate is not significantly deformed under high temperature, and the combination with the coating appears to be a straight line with no obvious boundaries or small gaps, indicating a good combination. As shown in Fig. 2(b), the bonding layer is compact and fine, consisting of Ti–Al intermetallic compound, which effectively protects the matrix alloy and achieves the purpose of surface modification. However, the outer coating structure contains numerous holes and has poor density. Additionally, multiple cracks are present within the coating, extending from the surface to the substrate. These issues greatly diminish the overall integrity of the coating. The volume shrinkage of the liquid phase and the solid phase, due to the different physical properties of TA15 titanium alloy and pure aluminum, results in a restraining stress on the surrounding tissue. When the coating is air-cooled, this stress exceeds its limit, leading to the formation of cracks. These cracks greatly affect the protective effect of the coating. Fig. 3 shows the microstructure of the sample when a certain intensity of alternating electromagnetic field is applied during the solidification process of the coating. From Fig. 3(a), it can be observed that the microstructure of the outer coating is improved, with fewer holes and increased density. The number of cracks is significantly reduced, although there are still a small number of longitudinal cracks perpendicular to the coating. In the alternating electromagnetic field, the molten coating experiences periodic changes in the electromagnetic force F. This continuous electromagnetic force F induces a contactless stirring effect on the coating. It enhances the convection intensity between the coating and the substrate, promoting the diffusion rate and material exchange between the atoms. It also fills the gaps that occur during solidification and contraction, effectively preventing the generation and growth of cracks in the coating. Additionally, the electromagnetic field has a thermal effect on the solidification process of the coating. The Joule heat Qj, which represents this thermal effect, is expressed in Eq. (1). Here, j denotes the density of the current passing through the coating and σ represents the conductivity of the alloy [31–33]. The thermal effect reduces the temperature gradient of the coating, leading to a more homogeneous solute field and temperature field from outside to inside. As a result, the possibility of stress concentration is reduced, and the number of cracks is controlled. However, it should be noted that the effectiveness of the alternating electromagnetic field is limited. Consequently, complete elimination of coating cracks is not achieved, and the outer coating may still contain holes and have a relatively loose structure [34,35].

$$Q_j = j^2/\sigma \tag{1}$$

Electromagnetic stirring technology is commonly employed in the metal solidification process. In this experiment, a stainless-steel generator is utilized, which is wrapped with a working coil. Upon connection to an AC power supply, the coil generates alternating electromagnetic fields within its hollow interior. These alternating electromagnetic fields act upon the coated melt. As the metal melt enters the magnetic field, the magnetic field lines are cut, resulting in the generation of induced current within the melt. The interaction between the induced current and the magnetic field produces an electromagnetic force of a certain intensity [36]. Since the alternating current undergoes periodic changes, the size and direction of the magnetic field also change periodically. As a result, electromagnetic stirring of the coated melt is achieved without the need for direct contact with the coating, thereby avoiding potential contamination. Electromagnetic stirring has several effects on the metal coating melt. Firstly, it promotes strong convection, leading to the homogenization of particle distribution and the reduction of both micro-segregation and macro-segregation of elements. The interaction between the coated melt and induced current, as well as the Lorentz force generated by the magnetic field, enhances periodic convection, alters the melt flow, and accelerates the diffusion rate between atoms. Specifically, the aluminum atoms within

Table 1
The main process parameters of HIP.

Temperature(°C)	Holding time (H)	Vacuum degree/P	Pressure(MPa)	Supercharging time(Min)
600	0.5	100	30	60
800	0.5	100	30	60

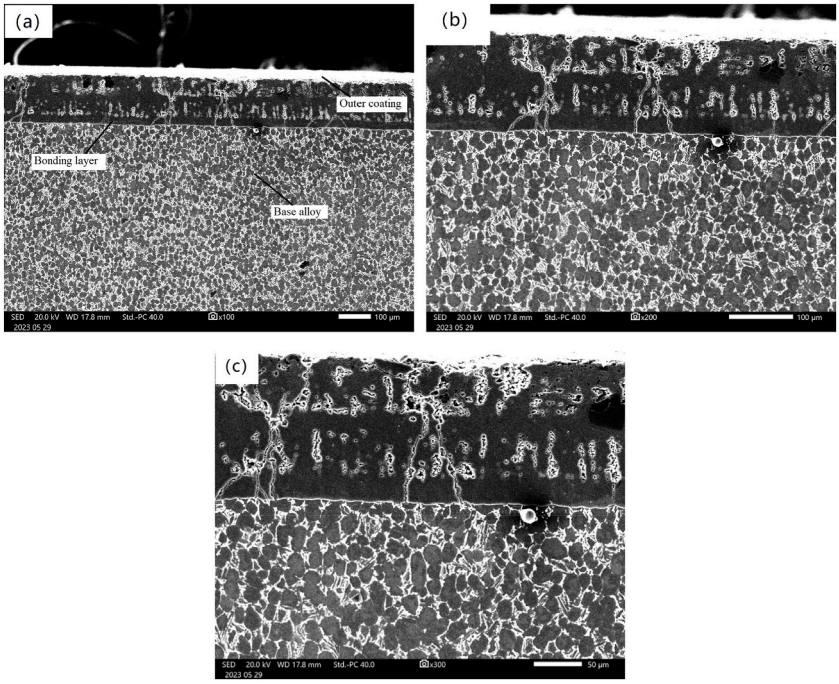

Fig. 2. Microstructure of traditional HDA coating. (a) 100 × (magnification), (b) 200 × , and (c) 300 × .

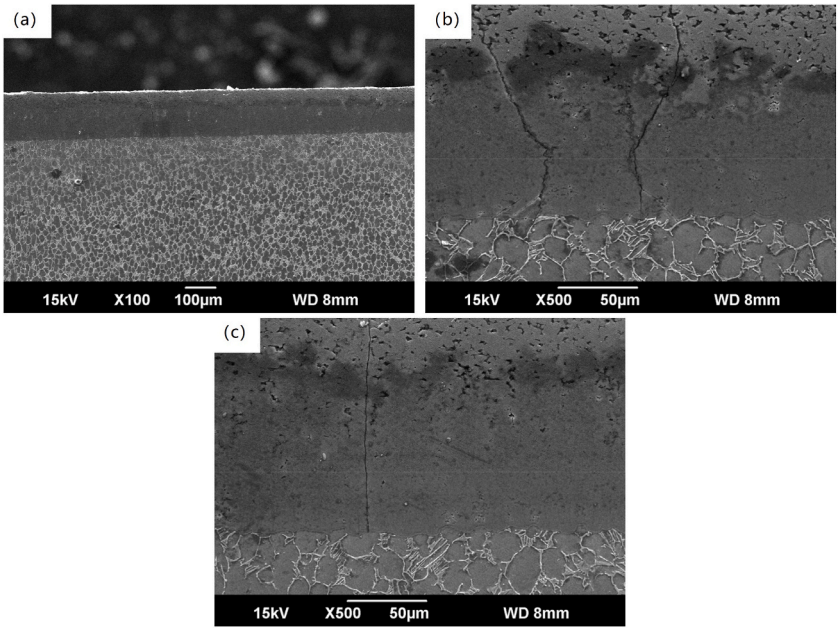

Fig. 3. Microstructure of HDA coating cooled in electromagnetic field. (a) 100 × , (b) 500 × , and (c) 500 × .

the outer coating move towards the titanium alloy matrix, resulting in a more dispersed and uniform distribution of elements. As solidification progresses, the Lorentz force fills the gaps formed during solidification shrinkage, optimizing the feeding channel. This reduces pore formation and partially inhibits the occurrence of hot cracks in the coating. Additionally, electromagnetic stirring refines the grain and improves the coating structure. Under the influence of the Lorentz force, the liquid metal flow experiences shear force during coating solidification, causing the crushing of coarse dendrites and dendrite tips that are difficult to flow. The resulting small dendrite fragments serve as new nucleation centers, increasing the nucleation rate and refining the grains. Furthermore, the alternating electromagnetic field has a thermal effect on the coating melt. The induced current passes through both the coating and the base

alloy, converting electrical energy into heat energy. This thermal effect lowers the melt temperature at the solidification front, reduces the overall temperature gradient of the coating, and enhances mass and heat transfer between materials. The rapid solidification of the traditional hot-dip aluminum coating in the air, combined with the different thermal expansion coefficients of aluminum and titanium alloy, leads to a large temperature gradient from the outside to the inside during the cooling process. This temperature gradient is one of the main factors contributing to the formation of cold cracks in the coating. However, the thermal effect of alternating electromagnetic field can stabilize the temperature field and solute field during the solidification process of the coating. This reduces the temperature gradient from the outside to the inside, resulting in a decrease in stress concentration and cracking sensitivity. As a result, the number of cold cracks and holes is reduced [37,38].

The microstructure of the 600 °C hot isostatic magnetic cold and hot dip aluminum coating is depicted in Fig. 4. The coating exhibits a gradient form, with the outer coating and binding layer arranged sequentially from the outside to the inside. The outermost pure aluminum layer is no longer present. The outer surface of the coating displays noticeable depressions and significant local deformations, leading to increased surface roughness and compromised surface quality. Longitudinal cracks are observed in the outer coating, running from the outermost side to the alloy matrix, along with transverse cracks parallel to the coating. The bonding layer, although relatively dense, also contains a certain number of longitudinal cracks. Moreover, the thickness of the bonding layer is significantly higher than that of traditional air cooling and magnetic cooling styles. At the holding temperature of 600 °C, the influence of equal pressure becomes more prominent. The outer surface of the coating exhibits fractures, with pressure serving as the driving force for the growth of transverse cracks. Additionally, a portion of the outer layer and the original binding layer transform into a thicker binding layer, resulting in a decrease in the quality of the outer surface and outer coating, and an increase in the thickness of the binding layer [39–41].

The microstructure of the 800 °C hot isostatic magnetic cold and hot dip aluminum coating is depicted in Fig. 5. The gradient morphology of the coating remains unchanged, exhibiting a uniform and refined microstructure with no apparent penetrating cracks observed. Hot isostatic pressing alters the cooling process of the hot dip aluminum coating under alternating electromagnetic field conditions. The application of high temperature and pressure facilitates enhanced material exchange between the coating and matrix, leading to improved bonding between aluminum atoms and titanium atoms within intermetallic compounds. Consequently, this significantly enhances the surface properties of the matrix alloy. Moreover, elevated temperatures promote thermochemical reactions between the coating and substrate alloy while simultaneous application of isostatic pressure promotes mutual diffusion of atoms. This results in a substantial migration of aluminum atoms towards the substrate, triggering a series of thermochemical reactions that effectively prevent crack formation. Under high temperature and pressure conditions, any loose structure present on the outer layer undergoes repair as shrinkage and porosity are filled without significant presence of voids or bubbles being detected. Furthermore, there becomes less distinction between the binding layer and outer coating as both achieve true metallurgical connection through dense organization [42,43]. Overall, hot isostatic pressing effectively enhances comprehensive properties of magnetic cold and hot dip aluminum coatings on titanium alloy surfaces.

Under the influence of high temperature and isostatic pressure in all directions, the defects in the hot isostatic magnetic cold and

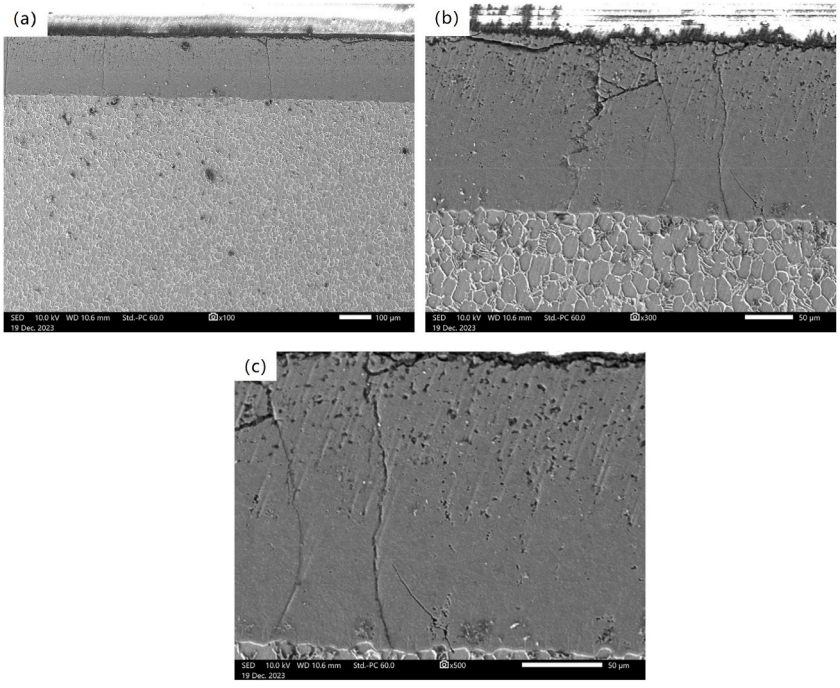

Fig. 4. The microstructure of the 600 °C HIP magnetic cold and hot dip aluminum coating. (a) 100 × , (b) 300 × , and (c) 500 × .

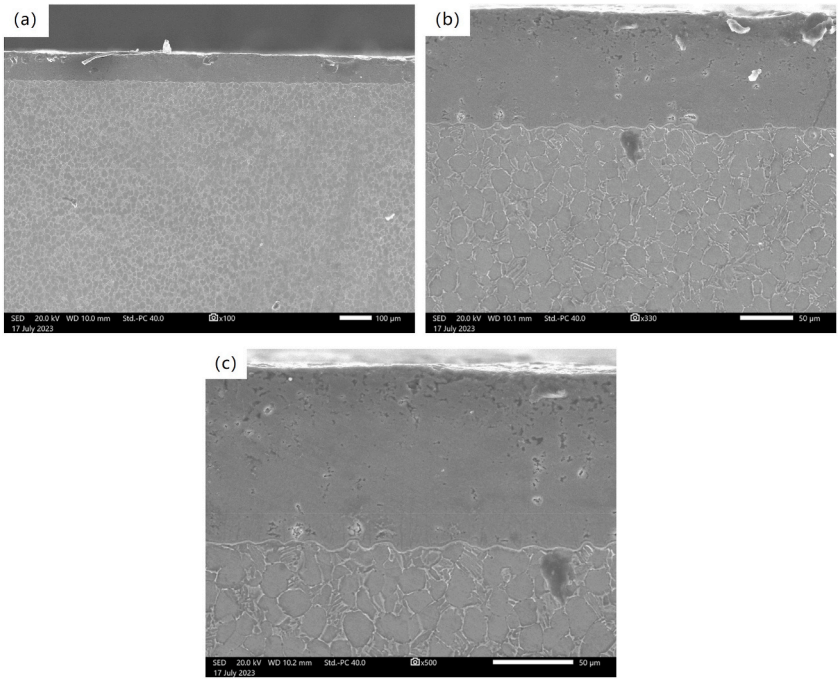

Fig. 5. The microstructure of the 800 °C HIP magnetic cold and hot dip aluminum coating. (a) 100 × , (b) 330 × , and (c) 500 × .

hot dip aluminum coating are repaired. The schematic diagram of its action principle is shown in Fig. 6. The entire process can be divided into three stages: material particle rearrangement, macroscopic plastic deformation, and diffusion creep. Temperature and pressure promote material particle rearrangement, leading to an improvement in the density of the coating. As temperature and pressure increase, the material surrounding the holes and cracks undergoes plastic deformation due to the stress gradient, facilitating the closure of the holes and the repair of the cracks. Consequently, the area fraction of the holes in the tissues significantly decreases. When temperature and pressure continue to rise, the stage of diffusion creep occurs. This stage involves complex physical and thermochemical reactions, with intensified interatomic diffusion. As a result, the microstructure and properties of the coating undergo changes without causing damage to the substrate and coating [44]. In the hot isostatic pressing process, temperature and pressure have a significant impact on metal alloys. Insufficient temperature prevents material particle rearrangement, and pressure alone is not a strong enough driving force. On the other hand, excessively high temperature can lead to excessive growth of the coating tissue, which can adversely affect its mechanical properties. Similarly, excessive pressure may cause damage to the outer surface structure of the coating. When the temperature is set at 600 °C and the holding pressure at 30 MPa, it is considered relatively low for both the alloy matrix and the coating, making the role of pressure more prominent. The process is only in the stage of particle rearrangement or macro plastic deformation, and there is a certain mutual diffusion between atoms, which can repair some small holes, but it is powerless for larger cracks. At the same time, the pressure provides the driving force for the cold deformation, breaks the surface topography of the coating, and has no obvious effect on the elimination of the defects such as holes and cracks of the coating in direct contact with the pressure. When the holding temperature is 800 °C, the process enters the stage of diffusion creep. High temperature

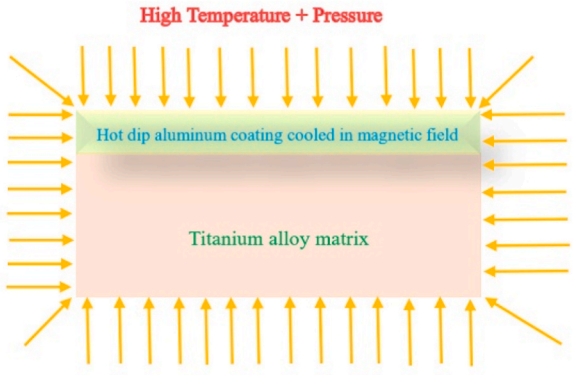

Fig. 6. Schematic diagram of principle of HIP magnetic cold and hot dipping aluminum coating.

aggravates the degree of diffusion between atoms, and the degree of creep deformation is much greater than the plastic deformation. Ti atoms and Al atoms first move to the center direction of cracks and holes under the driving force, repairing the defects of the coating.

3.2. Phase analysis

Fig. 7 presents a comparative analysis of X-ray diffraction for three different hot dip aluminum coating processes applied to the surface of TA15 titanium alloy. In the traditional hot-dip aluminum coating, the sample surface mainly consists of $TiAl_3$, AlV_3, Al_2O_3, and pure Al, which does not participate in the reaction. The solidification mode of intermetallic compounds in the absence of other external fields is as follows: Ti+3Al→$TiAl_3$, Al+3 V→AlV_3. The types of intermetallic compounds are limited, and Al_2O_3 is formed through the solidification of elemental Al and O elements in the air. The solidification mode is as follows: 2Al+3O→Al_2O_3. Additionally, some elemental pure Al directly solidifies to form a pure Al layer, which emerges as the outermost layer of the coating, thereby reducing the surface properties of the underlying titanium alloy. Apart from $TiAl_3$, Al_2O_3, and pure Al, the coating structure solidified in the alternating electromagnetic field primarily consists of $Ti_{0.8}Al_2V_{0.2}$, Ti_5Al_{11}, Ti_2Al_5, Ti_3Al_5, and Ti_3Al. Under the influence of the alternating electromagnetic field, AlV_3 combines with Ti atoms to form $Ti_{0.8}Al_2V_{0.2}$. The formation of various intermetallic compounds enhances the performance of the hot-dip aluminum coating. The main constituents of the 800 °C hot isostatic magnetic cold hot dip aluminum coating include $TiAl_3$, $Ti_{0.8}Al_2V_{0.2}$, Ti_5Al_{11}, Ti_2Al_5, Ti_3Al_5, and the new phases AlV and TiAl. The isostatic pressure exerted on each phase promotes the mutual diffusion of atoms and accelerates material exchange. This pressure also facilitates the conversion of Ti_3Al to TiAl and the formation of a more stable new phase, AlV. As a result, he pure Al component disappears, and all elements form certain compounds, hereby further improving the overall properties of the magnetic cold and hot aluminum dipping coating. The complex physical and thermochemical reactions promoted the binding of elemental Al and Ti atoms to form a new stable intermetallic compound and promoted the transformation of Ti_3Al to TiAl. The precipitation mode and solidification mode were AlV_3→Al+3 V, Al + V→AlV.

Fig. 8 and Table 2 present the EDS spectrum analysis results of the conventional hot-dipped aluminum coating on the surface of the titanium alloy. The error of the measured data is controlled within ±0.5, and the non-metallic element content error is large, which is not discussed in this experiment. The analysis reveals that the coating primarily consists of titanium (Ti), aluminum (Al), and vanadium (V) elements. Specifically, points 1 and 2 represent the outer layer of the coating, point 5 represents the matrix titanium alloy, point 3 represents the transition area between the binding site and the outer coating, and point 4 represents the binding site of the coating. During the dipping and plating process, the diffusion of Al element towards the substrate is prominent, resulting in a gradual decrease in the Ti content from the inside to the outside of the coating, and a corresponding decrease in the Al content from the outside to the inside. The atomic ratio of Ti and Al elements in the outer coating is approximately 1:3, while the atomic ratio at the binding site is approximately 1:1.5, indicating insufficient atom exchange between the coating and the substrate, leading to poor coating quality. On the other hand, Fig. 9 and Table 3 demonstrate the EDS spectrum analysis of the cooled hot-dip aluminum coating in an electromagnetic field. Point 2 represents the outer coating and point 3 represents the joint between the coating and the substrate. The atomic ratio of Ti and Al elements in the outer coating and the joint is approximately 1:1.6. Comparing it with the traditional hot-dipped aluminum coating, the atomic exchange between Ti and the substrate is more complete in the presence of the electromagnetic field at high temperature. The Ti element diffuses towards the coating direction, while the Al element diffuses more vigorously towards the substrate direction.

Fig. 10 and Table 4 present the EDS spectrum analysis of the hot isostatic pressing hot dip aluminum coating at 600 °C. The atomic ratio of Ti and Al elements in both the outer coating and the binding layer is approximately 1:1.8, indicating consistency. The equal pressure and high temperature in all directions facilitate the diffusion of Al elements towards the matrix, resulting in a relatively uniform distribution of elements in the coating. On the other hand, Fig. 11 and Table 5 demonstrate the EDS analysis of the hot isostatic pressing hot dip aluminum coating at 800 °C. The atomic ratios of Ti and Al elements in the outer layer of the coating and the joint are 1:1.8 and 1:1.2, respectively. Under the influence of high temperature and high pressure, the Al element at the coating joint diffuses more vigorously towards the matrix. As a result, the Ti–Al atomic ratio approaches 1:1, promoting the formation of various high-performance intermetallic compounds and enhancing the overall coating performance [45–47].

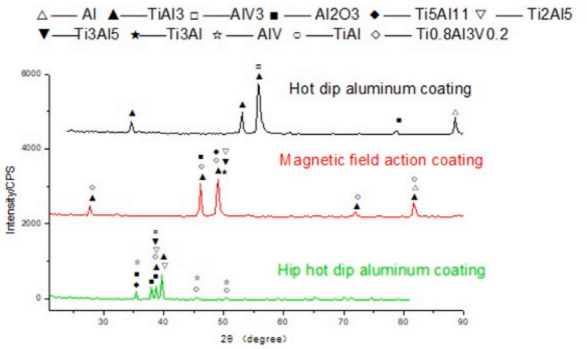

Fig. 7. XRD analysis of the coating.

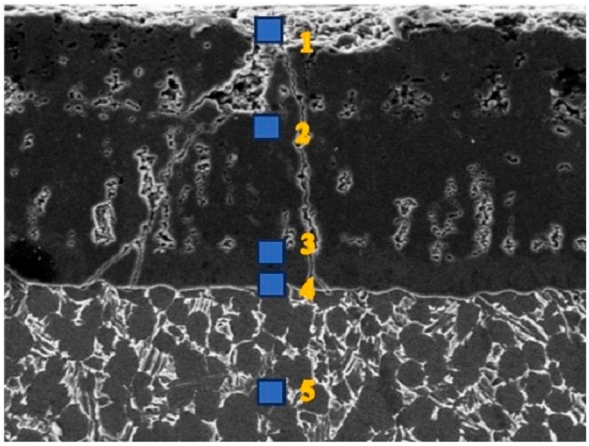

Fig. 8. EDS spectrum analysis of HDA coating.

Table 2
EDS spectra comparison of HAD coating.

Mass%	Ti	Al	V	other	Total
001	19.90	76.60	0.3	3.2	100.00
002	29.80	66.10	0.9	3.2	100.00
003	33.90	60.80	0.7	4.6	100.00
004	37.55	56.15	1.5	4.8	100.00
005	84.50	8.4	1.3	5.8	100.00

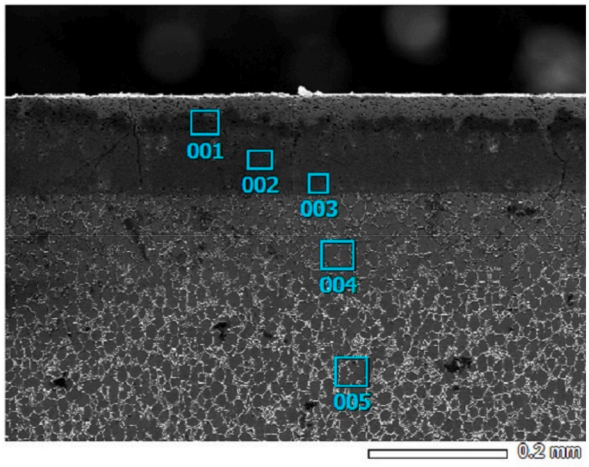

Fig. 9. EDS spectrum analysis of HDA coating cooled in electromagnetic field.

Table 3
EDS spectrum comparison of HDA coating cooled in electromagnetic field.

Mass%	Ti	Al	V	other	Total
001	37.64	60.33	0.03	2.0	100.00
002	37.96	60.02	0.02	2.0	100.00
003	38.08	59.78	0.14	2.0	100.00
004	86.58	7.58	0.14	5.7	100.00
005	86.92	7.24	0.14	5.7	100.00

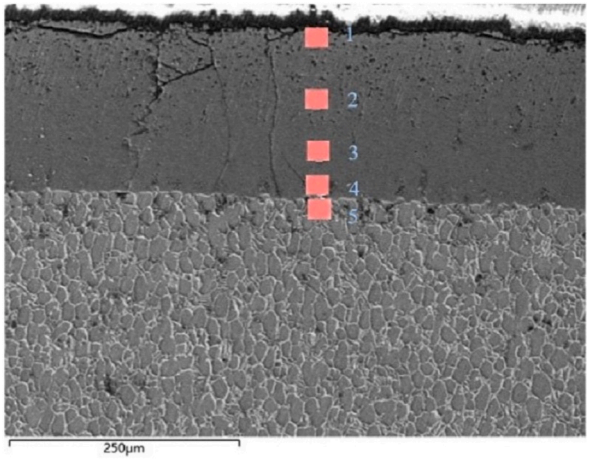

Fig. 10. EDS spectrum analysis of the 600 °C HIP magnetic cold and hot dip aluminum coating.

Table 4
EDS spectrum comparison of the 600 °C HIP magnetic cold and hot dip aluminum coating.

Mass%	Ti	Al	V	other	Total
001	34.8	62.3	1.1	1.8	100.00
002	35.3	61.9	1.0	1.8	100.00
003	35.2	62.3	0.7	1.8	100.00
004	35.7	62.1	0.4	1.8	100.00
005	92.3	8.0	1.2	5.7	100.00

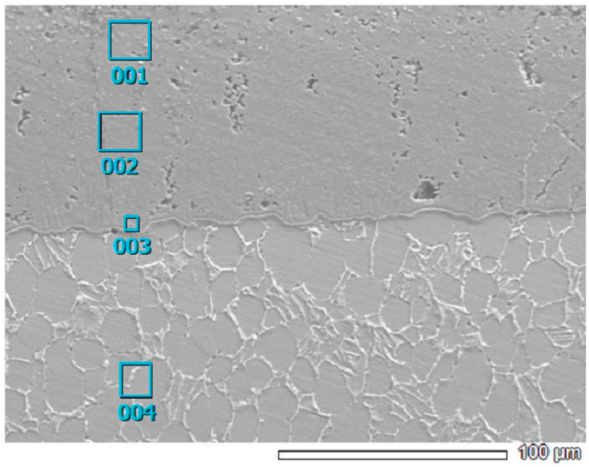

Fig. 11. EDS spectrum analysis of the 800 °C HIP magnetic cold and hot dip aluminum coating.

Table 5
EDS spectrum comparison of the 800 °C HIP magnetic cold and hot dip aluminum coating.

Mass%	Ti	Al	V	other	Total
001	37.07	60.98	0.25	1.7	100.00
002	36.64	61.13	0.53	1.7	100.00
003	43.21	54.65	0.44	1.7	100.00
004	88.34	9.79	0.17	5.7	100.00

3.3. Microhardness

The microhardness distribution of the hot-dipped aluminum coating on the surface of TA15 titanium alloy with three different processes is illustrated in Fig. 12. The measured data is the average of the points taken, the error can be controlled within ±2. The highest hardness of the coating is observed near the coating junction and gradually decreases towards the outer part of the coating. The maximum hardness at the joint of the traditional hot-dip aluminum coating can reach 543.3HV. In this area, certain intermetallic compounds are present, which enhance the hardness of the titanium alloy matrix. The surface hardness of the coating solidified in the alternating electromagnetic field is generally lower compared to the traditional process, with a maximum hardness of 510.8HV, approximately 6 % lower than the traditional process. This could be attributed to the thermal effect of the alternating electromagnetic field, which slows down the cooling rate of the coating. On the other hand, the 800 °C hot isostatic magnetic cold and hot dip aluminum coating exhibits higher hardness than the other two coatings in the same area, with a joint hardness of up to 722.4HV. The hot isostatic pressing process leads to coating remelting, resulting in a denser structure and significantly reduced defects. This allows better combination of aluminum atoms and matrix titanium atoms to form intermetallic compounds, which greatly enhance the hardness of the coating [48]. Therefore, the microhardness of hot isostatic magnetic cold and hot dip aluminum coating stands out as the most prominent among the three different processes.

4. Conclusion

The effect of hot isostatic pressing (HIP) on the microstructure and properties of hot dip aluminum coating cooled in a magnetic field was investigated in this study. The microstructure and element distribution of three different coatings were analyzed, and the microhardness of the coatings at various positions was tested. The main conclusions are drawn as below,

(1) The TA15 titanium alloy traditional hot dip aluminum air-cooled coating exhibits a gradient structure with numerous holes and poor density in the outer coating structure. During the solidification process of the coating, applying a certain intensity of alternating electromagnetic field enhances the microstructure by inhibiting hole formation, increasing microstructure density, and significantly reducing crack occurrence. However, longitudinal cracks perpendicular to the coating still exist.
(2) At the holding temperature of 600 °C, the influence of equal pressure becomes more prominent. The outer surface of the coating exhibits fractures. Additionally, a portion of the outer layer and the original binding layer transform into a thicker binding layer, resulting in a decrease in the quality of the outer surface and outer coating, and an increase in the thickness of the binding layer. The outermost pure aluminum layer in the 600 °C hot isostatic magnetic cold and hot dip aluminum coating disappears, resulting in noticeable depressions on the outer surface that affect its quality.
(3) At 800 °C hot isostatic magnetic cold and hot dip aluminum coating exhibits a uniform and fine microstructure without any obvious penetrating cracks. After hot isostatic pressing at 800 °C, Al element diffuses more strongly towards the matrix at binding points of the coating. This diffusion results in a Ti–Al atomic ratio closer to 1:1 and leads to various high-performance intermetallic compounds forming within the coating. Consequently, this enhances overall performance. The surface hardness of coatings solidified using an alternating electromagnetic field generally tends to be lower compared to traditional processes. However, coatings produced through 800 °C hot isostatic magnetic cold and hot dip aluminum method exhibit higher hardness than those from other two processes within similar areas; reaching up to 722.4HV.

Data availability

The data that support the findings of this study are available from the corresponding author upon reasonable request.

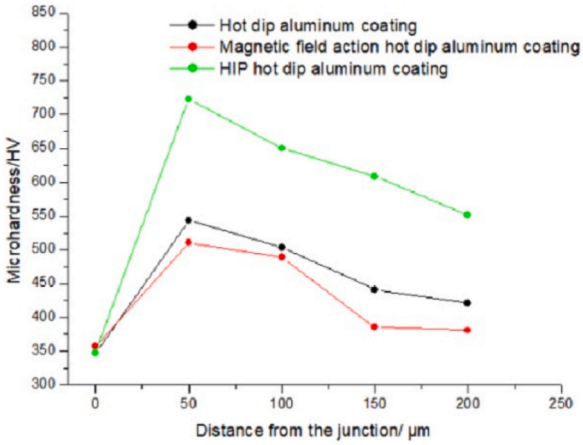

Fig. 12. Microhardness analysis of the coating.

Funding

The author thanks the financial support provided by the Chinese Aeronautical Establishment (GrantNo. 2023Z053158001), and the Material Corrosion and Protection Key Laboratory of Sichuan Province(GrantNo. 2023CL21), and the Chengdu Aeronautic Polytechnic (GrantNo. ZZX0623066), and Chengdu Aviation Industry Development and Cultural Construction Research Center (grant No. CAIACDRCXM2024-13).

CRediT authorship contribution statement

Li Yong: Writing – review & editing, Writing – original draft. **Xu Wei:** Writing – review & editing, Writing – original draft, Funding acquisition. **Bai Jingfei:** Investigation, Data curation. **Su Qing:** Funding acquisition. **Xu RuTao:** Software, Resources. **Liu Hong:** Visualization, Software. **Dan Yu:** Resources, Investigation.

Declaration of competing interest

The authors declare that they have no known competing financial interests or personal relationships that could have appeared to influence the work reported in this paper.

References

[1] Lihua Fu, Wei Han, Karin Gong, Sven Bengtsson, Chaofang Dong, Zhao Lin, Zhiling Tian, Microstructure and tribological properties of Cr3c2/Ni3al Composite materials prepared by hot isostatic pressing (hip), Mater. Des. 115 (2017) 203–212.
[2] J. Kadkhodapour, A. Butz, S. Ziaei Rad, Mechanisms of void formation during tensile testing in a commercial, dual-phase steel, Acta Mater. 59 (7) (2011) 2575–2588.
[3] A. Rajabi, M.J. Ghazali, A.R. Daud, Chemical composition, microstructure and sintering temperature modifications on mechanical properties of tic-based cermet – a review, Mater. Des. 67 (2015) 95–106.
[4] Z.G. Zhang, Y.P. Peng, Y.L. Mao, C.J. Pang, L.Y. Lu, Effect of hot-dip aluminizing on the oxidation resistance of Ti–6al–4v alloy at high temperatures, Corrosion Sci. 55 (2012) 187–193.
[5] A. Schneider, V. Avilov, A. Gumenyuk, M. Rethmeier, Laser beam welding of aluminum alloys under the influence of an electromagnetic field, Phys. Procedia 41 (2013) 4–11.
[6] Hui Zhang, Zhaolin Zhan, Xingbo Liu, Electrophoretic deposition of (Mn,Co)3o4 spinel coating for solid oxide fuel cell interconnects, J. Power Sources 196 (19) (2011) 8041–8047.
[7] Xiang-Yu Ma, Tian-Cheng Ma, Ya-Fei Feng, Geng Xiang, Wei Lei, Da-Peng Zhou, Hai-Long Yu, Liang-Bi Xiang, Lin Wang, Promotion of osteointegration under diabetic conditions by a silk fibroin coating on 3d-printed porous titanium implants via a ros-mediated nf-κb pathway, Biomed. Mater. 16 (3) (2021) 035015.
[8] Yang Li, Xiufang Cui, Guo Jin, Zhaobing Cai, Na Tan, Bingwen Lu, Yu Yang, Zonghong Gao, Jinna Liu, Influence of magnetic field on microstructure and properties of tic/cobalt-based composite plasma cladding coating, Surf. Coating. Technol. 325 (2017) 555–564.
[9] Stefan Heinz, Frank Balle, Guntram Wagner, Dietmar Eifler, Analysis of fatigue properties and failure mechanisms of Ti6al4v in the very high cycle fatigue regime using ultrasonic technology and 3d laser scanning vibrometry, Ultrasonics 53 (8) (2013) 1433–1440.
[10] Richard A. Barrett, Padraic E. O'Donoghue, Sean B. Leen, A physically-based constitutive model for high temperature microstructural degradation under cyclic deformation, Int. J. Fatig. 100 (2017) 388–406.
[11] S.N. Li, Influence of magnetic field on micro-structure andperformance of feconicro, Sb High Entropy Alloy Coating in Plasma Cladding. D (2022).
[12] L. Chen, Experimental and Simulationstudy on 304 Stainless Steel Powder Laser Cladding Assisted by Coupled Field of Electric and Magnetic. D (2018).
[13] M. Gatzen, Z. Tang, F. Vollertsen, Effect of electromagnetic stirring on the element distribution in laser beam welding of aluminium with filler wire, Phys. Procedia 12 (2011) 56–65.
[14] Michael Hauser, Marco Wendler, Olga Fabrichnaya, Olena Volkova, Javad Mola, Anomalous stabilization of austenitic stainless steels at cryogenic temperatures, Mater. Sci. Eng., A 675 (2016) 415–420.
[15] Marcel Bachmann, Vjaceslav Avilov, Andrey Gumenyuk, Michael Rethmeier, About the influence of a steady magnetic field on weld pool dynamics in partial penetration high power laser beam welding of thick aluminium parts, Int. J. Heat Mass Tran. 60 (2013) 309–321.
[16] Fengcang Ma, Tianran Wang, Ping Liu, Wei Li, Xinkuan Liu, Xiaohong Chen, Deng Pan, Weijie Lu, Mechanical properties and strengthening effects of in situ (Tib +Tic)/Ti-1100 composite at elevated temperatures, Mater. Sci. Eng., A 654 (2016) 352–358.
[17] Xiao-na Peng, Hong-zhen Guo, Zhi-feng Shi, Chun Qin, Zhang-long Zhao, Microstructure characterization and mechanical properties of Tc4-dt titanium alloy after thermomechanical treatment, Trans. Nonferrous Metals Soc. China 24 (3) (2014) 682–689.
[18] K. Mori, Tomoyoshi Maeno, Hiroaki Yamada, Hayato Matsumoto, 1-Shot hot stamping of ultra-high strength steel parts consisting of resistance heating, forming, shearing and die quenching, Int. J. Mach. Tool Manufact. 89 (2015) 124–131.
[19] K. Mori, Smart hot stamping of ultra-high strength steel parts, Trans. Nonferrous Metals Soc. China 22 (2012) s496–s503.
[20] Y.X. Gao, Z.W. Ll, K. Liu, et al., Effect of post-treatment on microstructure and properties of Ti48ai2cr2nb alloy prepared by electron beam melting, Transa Ctions of Materials and Heat Reatment 44 (11) (2023) 101–106.
[21] S. Praveen, B.S. Murty, Ravi S. Kottada, Phase evolution and densification behavior of nanocrystalline multicomponent high entropy alloys during spark plasma sintering, JOM 65 (12) (2013) 1797–1804.
[22] Jithin Joseph, Peter Hodgson, Tom Jarvis, Xinhua Wu, Nicole Stanford, Daniel Mark Fabijanic, Effect of hot isostatic pressing on the microstructure and mechanical properties of additive manufactured alxcocrfeni high entropy alloys, Mater. Sci. Eng., A 733 (2018) 59–70.
[23] X.Y. Tian, J.X. Wel, H. Yan, et al., Effect of hot isostatic pressing on Microstructure,Room temperature and hightemperature mechanical properties of low-pressure casting We43 magnesium alloy, Trans. Mater. Heat Treat. 44 (10) (2023) 87–95.
[24] Y. Li, Effect of Alternating Electromagnetic Field on the Microstructure and Property of Vacuum Counter-Pressure Casting Aluminum Alloy. D (2013).
[25] N.D. Stepanov, N. Yu Yurchenko, D.V. Skibin, M.A. Tikhonovsky, G.A. Salishchev, Structure and mechanical properties of the alcrxnbtiv (X = 0, 0.5, 1, 1.5) high entropy alloys, J. Alloys Compd. 652 (2015) 266–280.
[26] X.T. Li, L.J. Huang, S.L. Wei, Q. An, X.P. Cui, L. Geng, Cycle oxidation behavior and anti-oxidation mechanism of hot-dipped aluminum coating on tibw/Ti6al4v composites with network microstructure, Sci. Rep. 8 (1) (2018) 5790.
[27] Abro, Muhammad Ali, Junhee Hahn, Dong Bok Lee, High temperature oxidation of hot-dip aluminized T92 steels, Met. Mater. Int. 24 (3) (2018) 507–515.
[28] Shanshan Sun, Qing Teng, Yin Xie, Liu Tong, Rui Ma, Jie Bai, Chao Cai, Wei Qingsong, Two-step heat treatment for laser powder bed fusion of a nickel-based superalloy with simultaneously enhanced tensile strength and ductility, Addit. Manuf. 46 (2021) 102168.
[29] Haonan Zheng, Chao Cai, Ruipeng Guo, Yusheng Shi, Diffusion bonding among hard alloy, tool steel, and alloy steel by hot isostatic pressing: interfacial microstructure and mechanical properties, Int. J. Refract. Metals Hard Mater. 118 (2024) 106478.

[30] R.P. Guo, M. Cheng, C.J. Zhang, J.W. Qiao, C. Cai, Q.J. Wang, D.S. Xu, L. Xu, R. Yang, Y.S. Shi, P.K. Liaw, Achieving superior fatigue strength in a powder-metallurgy titanium alloy via in-situ globularization during hot isostatic pressing, Scripta Mater. 228 (2023) 115345.
[31] Yi-da Chen, Yong Yang, Zhen-hua Chu, Xue-guang Chen, Lei Wang, Zhe Liu, Yan-chun Dong, Dian-ran Yan, Jian-xin Zhang, Zhi-long Kang, Microstructure and properties of Al2o3-zro2 composite coatings prepared by air plasma spraying, Appl. Surf. Sci. 431 (2018) 93–100.
[32] M. Palm, G. Sauthoff, Deformation behaviour and oxidation resistance of single-phase and two-phase L21-ordered Fe–Al–Ti alloys, Intermetallics 12 (12) (2004) 1345–1359.
[33] Fengyuan Shu, Binglin Zhang, Tao Liu, Shaohua Sui, Yuxin Liu, Peng He, Bin Liu, Binshi Xu, Effects of laser power on microstructure and properties of laser cladded cocrbfenisi high-entropy alloy amorphous coatings, Surf. Coating. Technol. 358 (2019) 667–675.
[34] Y.Z. Liu, L.H. Zhan, Q.Q. Ma, Z.Y. Ma, M.H. Huang, Effects of alternating magnetic field aged on microstructure and mechanical properties of Aa2219 aluminum alloy, J. Alloys Compd. 647 (2015) 644–647.
[35] T. Ben Britton, Soran Birosca, Michael Preuss, Angus J. Wilkinson, Electron backscatter diffraction study of dislocation content of a macrozone in hot-rolled Ti–6al–4v alloy, Scripta Mater. 62 (9) (2010) 639–642.
[36] Thorsten Heeling, Michael Cloots, Konrad Wegener, Melt pool simulation for the evaluation of process parameters in selective laser melting, Addit. Manuf. 14 (2017) 116–125.
[37] Yanyan Du, Yiping Lu, Tongmin Wang, Tingju Li, Guoliang Zhang, Effect of electromagnetic stirring on microstructure and properties of Al0.5cocrcufeni alloy, Procedia Eng. 27 (2012) 1129–1134.
[38] C. Tang, J.L. Tan, C.H. Wong, A numerical investigation on the physical mechanisms of single track defects in selective laser melting, Int. J. Heat Mass Tran. 126 (2018) 957–968.
[39] Xin Zhou, Xihe Liu, Dandan Zhang, Zhijian Shen, Wei Liu, Balling phenomena in selective laser melted tungsten, J. Mater. Process. Technol. 222 (2015) 33–42.
[40] Yufan Zhao, Yuichiro Koizumi, Kenta Aoyagi, Daixiu Wei, Kenta Yamanaka, Akihiko Chiba, Molten pool behavior and effect of fluid flow on solidification conditions in selective electron beam melting (sebm) of a biomedical Co-Cr-Mo alloy, Addit. Manuf. 26 (2019) 202–214.
[41] M. Dodaran, A. Hemmasian Ettefagh, S.M. Guo, M.M. Khonsari, W.J. Meng, N. Shamsaei, S. Shao, Effect of alloying elements on the Γ″ antiphase boundary energy in Ni-base superalloys, Intermetallics 117 (2020) 106670.
[42] Chu Lun Alex Leung, Sebastian Marussi, Robert C. Atwood, Michael Towrie, Philip J. Withers, Peter D. Lee, In situ X-ray imaging of defect and molten pool dynamics in laser additive manufacturing, Nat. Commun. 9 (1) (2018) 1355.
[43] Bi Zhang, Yongtao Li, Qian Bai, Defect Formation mechanisms in selective laser melting: a review, Chin. J. Mech. Eng. 30 (3) (2017) 515–527.
[44] Parastoo Jamshidi, Miren Aristizabal, Weihuan Kong, Victor Villapun, Sophie C. Cox, Liam M. Grover, Moataz M. Attallah, Selective laser melting of Ti-6al-4v: the impact of post-processing on the tensile, fatigue and biological properties for medical implant applications, Materials 13 (12) (2020) 2813.
[45] Hengfeng Gu, Haijun Gong, Deepankar Pal, Khalid Rafi, Brent Stucker, Influences of Energy Density on Porosity and Microstructure of Selective Laser Melted 17-4ph Stainless Steel, 2013.
[46] Tian Yulu, Jiang Yuan, Liu Qi, Xu Dingxue, Shoudong, Zhao, Effect of hot isostatic pressing on microstructure and mechanical properties of clam steel produced by selective laser melting, Landsc. Urban Plann. (2019).
[47] Erica Liverani, Adrian H.A. Lutey, Alessandro Ascari, Alessandro Fortunato, The effects of hot isostatic pressing (hip) and solubilization heat treatment on the density, mechanical properties, and microstructure of austenitic stainless steel parts produced by selective laser melting (slm), Int. J. Adv. Des. Manuf. Technol. 107 (1) (2020) 109–122.
[48] Jianglong Zhang, Zheng Zhang, Zihua Zhao, Qunpeng Zhong, Baohua Nie, Research on the healing behavior of the millimeter-sized cavity defect inside the superalloy by hot isostatic pressing, Mater. Lett. 235 (JAN.15) (2019) 57–60.